A Mixed Framework to Support Heterogeneous Collection Asset Scheduling

Jean Berger
Defence Research Development
Canada - Valcartier
Québec, PQ, Canada
jean.berger@drdc-rddc.gc.ca

Moufid Harb
Larus Technologies
Ottawa, ON, Canada
moufid.harb@larus.com

Ibrahim Abualhaol
Larus Technologies
Ottawa, ON, Canada
ibrahim.abualhaol@larus.com

Alexander Tekse
Larus Technologies
Ottawa, ON, Canada
alex.teske@larus.com

Rami Abielmona
Larus Technologies
Ottawa, ON, Canada
rami.abielmona@larus.com

Emil Petriu
University of Ottawa
Ottawa, ON, Canada
petriu@uottawa.ca

ABSTRACT

A new framework[1] mixing evolutionary approach, discrete-event simulation and deep neural networks is proposed to achieve multi-asset collection/image acquisition scheduling in a surveillance context. It combines an extended graph-based hybrid genetic algorithm (GA) used for satellite image acquisition scheduling, with a predictive simulation-based deep neural network and knowledge-based capabilities to solve an heterogeneous collection asset scheduling problem. Plan execution simulation and neural networks predict track trajectories target behaviors. In contrast, a knowledge-based approach is used to estimate target identification. Both assessments are exploited to instantiate key solution quality parameters of a generalized decision model aimed at maximizing task collection value subject to a variety of collector capacity constraints. The mixed framework departs from basic point target/area coverage task modeling, introducing tracking and identification tasks while expanding resource allocation to various space, air and ground-based deployable image acquisition/collection asset types.

CCS CONCEPTS

• **Mathematics of computing → Evolutionary algorithms**

KEYWORDS

Collection scheduling, simulation, genetic algorithm, deep neural networks

1 INTRODUCTION

Image acquisition scheduling involving low-density high demand collection assets is key to maintain persistent situational awareness. Pervasive in many domains including Earth observation and, defence and security intelligence, surveillance and reconnaissance (ISR) missions, it aims at maximizing collection information gain searching to bridge the gap between information need and information gathering. As typically shown through constrained multi-satellite scheduling [1]-[3], proposed approaches designed to maximize collection gain are often limited to a single type of homogeneous collection assets, basic task representation (e.g. point/area coverage) and simplistic collection task plan performance modeling. Recent efforts have been very modest in concurrently accounting for heterogeneous collection assets and task diversity or realistically considering performance modeling complexity in evaluating collection task plans.

In this paper, a new framework harnessing evolutionary approach, discrete-event simulation, machine learning and knowledge-based systems is proposed to solve the multi-asset collection/image acquisition scheduling problem to support surveillance missions. It mixes an extended graph-based hybrid genetic algorithm used for satellite image acquisition scheduling, with a predictive simulation-based deep neural network and knowledge-based capabilities to allocate heterogeneous collection assets to various imaging tasks to maximize expected collection value subject to a variety of collector capacity constraints. The framework relies on a predictive simulation-based deep neural network capability to generate and select tracks/behaviors and a predefined knowledge-based approach in feeding tracking and identification task decision model performance parameters. The promoted approach departs from basic point target/area coverage task modeling, introducing tracking and identification tasks while expanding resource allocation to various space, air and ground - based deployable image acquisition/collection asset types such as satellite, unmanned aerial/ground vehicles (UAVs, UGVs) or aircrafts to support surveillance or imagery intelligence missions.

The remainder of the paper is structured as follows. Section 1 introduces the multi-asset collection/image acquisition scheduling problem. It highlights the main problem features and outlines the underlying mathematical decision model. Section 3 describes the

GECCO'19 Companion, July 13-17, 2019, Prague, Czech Republic

ACM ISBN 978-1-4503-6748-6/19/07…$15.00
https://doi.org/10.1145/3319619.3326889

hybrid genetic algorithms proposed to solve the problem. The predictive simulation-based deep neural network and knowledge-based approaches used to characterize tracking and identification tasks in informing the decision model with performance parameters on task plans are briefly described in section 4. A scenario is briefly illustrated in section 5. A summary and future work directions are finally given in section 6.

2 PROBLEM DESCRIPTION

Given a set of information requests (point or areas of interest to be observed) properly translated into weighted tasks, the single episode (static) multi-asset image acquisition scheduling problem consists in allocating collection assets (collectors) to observation tasks (imaging opportunities) over a predetermined time horizon to maximize overall expected collection value, subject to a variety of constraints. Typical constraints refer to conditions imposed on mission, task, collector, communication, on-board resource capacity (e.g. energy and memory), temporal activities (e.g. imaging opportunity transition, imaging and task completion time windows), itinerary (e.g. duty cycle referring to maximum cumulative imaging time per cycle) and cost considerations respectively. A limited non-deterministic (observation outcome uncertainty) environment setting in which image acquisition (or observation outcome uncertainty) is characterized by a probability of successful observation is assumed to prevail, subject to resource contention (low-density, high demand assets) and high combinatorial complexity.

A request is characterized by an area of interest (AOI) to be covered (acquired). Two possible shapes of request defining either a point (spot) or a polygon are considered. A point of interest (POI) determines the center of an area to be imaged by a square shaped swath. The POI can be covered by a single collection asset visit whereas a wide area target generally depicted by a polygon often requires multiple-orbit visits to achieve full coverage. The task-dependent generation process producing image acquisition opportunity identifies all feasible task-collector schedules.

A directed acyclic graph representation is exploited to capture observation or collection opportunities (imaging opportunity selection) over a given vehicle tour (e.g. satellite orbit) as illustrated in Fig. 1. It implicitly reflects conflicting intra-tour opportunity transition constraints while implicitly imposing a partial temporal ordering over the collection opportunities, which considerably facilitates and speeds up sub-path reconstruction whenever needed. Such constraints comprise vehicle tour duration or itinerary path length and legal moves. Let R be the set of requests r with nominal value or priority V_{r0} referring to AOI A_r, and, R_ρ the set of complete/partial requests (tasks) visible on tour orbit ρ ($R_\rho \subseteq R$) matching sensor collection asset (vehicle) tour ρ

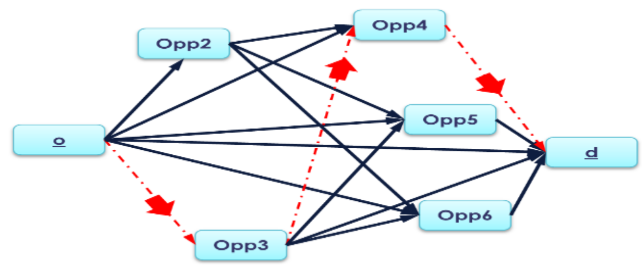

Figure 1: A collection network representation is used to capture collection path plans defining possible sequence of feasible observations (opportunities). A node reflects an imaging opportunity Opp whereas an arc translates legal transition between collections. A collector path plan is specified as a route/tour (dotted lines) in the collection graph. Artificial source o and destination d vertices bound the route.

capability (feasible matching), P_r the set of vehicle tour ρ having visibility on request/task r, O_ρ the set of opportunities o over vehicle tour ρ, and $O_{r\rho}$ the set of opportunities associated to request r on vehicle tour ρ, ($O_\rho = \cup_r O_{r\rho}$) covering area $A_{ro\rho}$ respectively. Opportunities are generated as feasible imaging options based on collection asset kinematics, on-board sensor characteristics and geometry. Each opportunity o related to request/task r under tour ρ involves by key parameters and measures of performance. Parameters include a look angle $\theta_{ro\rho}$, a time window defined by a start time $ts_{ro\rho}$, an end time $te_{ro\rho}$ and a duration $d_{ro\rho}$ respectively. Measures of performance alternately comprise covered area, estimated probability of successful observation $p_{ro\rho}$ accounting for outcome uncertainty (such as imperfect environmental/operating conditions or sensor failures), cost $cost_{ro\rho}$, and quality $q_{ro\rho}$. As a result, a task may require several visits to reach acceptable full or partial coverage. Following an observation, the collection asset then proceeds toward a transitioning phase performing a sequence of operations necessary to successfully initiate the next scheduled image acquisition. Set-up (e.g., sensor stabilization, start-up/shutdown) time and transition delay ultimately determines feasible moves and therefore, admissible imaging opportunity transitions. Collection asset resources are subject to a variety of constraints including duty cycle, memory storage and energy budget capacity for imaging and transition activities, as well as a financial budget. An integer binary decision variable $x_{ro\rho}$ associated to a node visit $o(r)$ on a task r defines a basic collector path's construct. Correspondingly, a path solution for collection route ρ includes vertex $o(r)$ if $x_{ro\rho}$=1. Hence, a feasible collector path solution may be built, navigating through the directed acyclic network, instantiating a sequence of decision variables.

Proposed collection asset tour graph representation generalizes satellite orbit/path collection network modeling presented in [4]. A satellite is replaced by a generic collection platform (vehicle) while an orbit corresponds to a legal tour or itinerary (e.g. an aircraft sortie), mostly subject to similar capacity and time constraints (e.g. energy, memory, transition). The proposed model maps a satellite platform orbit to a separate distinct tour/route whereas single tours (route/path) characterize other collection asset vehicle sorties over the problem time horizon. The objective consists of building a set of collection paths (tours), navigating through respective collection graphs and selecting high-payoff imaging opportunity nodes.

Extensions and novelty to the previous decision model [4] include:

- Multiple candidate tracking behaviors for a dynamic or moving target. It relies upon various feature models (such as threat and kinematic) and Monte Carlo simulation to generate likely trajectories generalizing basic coverage area imaging opportunity introducing the temporal dimension. Tracking generalizes basic target coverage accounting for the passage of time when generating feasible imaging opportunities, while considering multiple tracks at once. A cognitive map describing the single best or most likely tracks out of many, reflecting dynamic target position/behavior probability distribution, may be used to define a track area of interest and determine imaging opportunity measure of performance/quality of collection. Alternatively selecting the most likely track out of many, assuming deterministic point of interest evolution over time resulting in a single opportunity track area to image, could be optionally considered should probability distribution to support realistic simulation be unknown or unsatisfactorily modeled in order to simplify decision model complexity.
- Task identification based upon a customized user-defined domain-dependent knowledge-based classification system coupled to Monte Carlo simulations to estimate identity class probability distribution. In a maritime surveillance domain context, dark ship identification over a given area of interest constitutes a common classification task. Target threat/risk level (low, medium, high) or suspected illegal rendezvousing behavior classification (e.g. piracy, smuggling, and swarming) might represent alternate identification tasks. Sophisticated probabilistic classifiers exploiting deep learning coupled to Monte Carlo simulation are under development to better characterize and estimate probability distribution over possible candidate identity instances for selected identification tasks.
- Heterogeneous collection assets space-based, air-based (UAVs, aircrafts, copters) and ground-based (manned/unmanned vehicles) collectors may be combined to enrich intelligence, surveillance and reconnaissance (ISR) mission plans. Collection graph generation enabling construction of feasible collection path plans (sequence of imaging opportunities) is therefore asset-specific and constraint-dependent.

2.1 Decision Model

A mixed multi-asset collection scheduling framework to concurrently support coverage, tracking and identification tasking applied to a surveillance context is proposed. The underlying mathematical problem model expands from pure basic coverage tasks collection value characterization [4] to capture measures of performance featuring tracking an identification tasks drawn from simulation coupled to domain-dependent machine learning predictions and knowledge-based classification.

The main notations used to specify the problem model are specified as follows:

Parameters:

H: time horizon

Collection asset and resource constraints:

CA: set of heterogeneous collection asset platforms (e.g. earth observation satellites, UAVs, aircrafts, UGVs).

P : set of collection asset tours over period H

P_r: set of collection asset tours that can service task r. $P_r \subseteq P$

T_ρ: collection asset route/tour ρ duration

W_ρ : memory storage capacity over a collection asset tour ρ

E_ρ: energy capacity of collection asset tour ρ

Requests/tasks:

R: set of requests r. A request r defines a point target (spot) or a polygon area A_r to be covered. $R = R_{CVG} \cup R_{TRK} \cup R_{ID}$

R_{CVG}: set of basic coverage (point/area survey) request

R_{TRK}: set of tracking request

R_{ID}: set of identification request

A_r: area of interest (AOI) of request r

V_{r0}: nominal value of request r ranging over [0,1]

Imaging opportunities:

O_r: set of collection opportunities for task r

O_ρ: set of collection opportunities over collection asset route/tour ρ

$O_{r\rho}$: set of collection opportunities for request r over collection asset route/tour ρ

O: set of all collection opportunities

$\theta_{ro\rho}$: pointing/look angle for imaging task r opportunity o on collection asset tour ρ

$ts_{ro\rho}$: imaging task r opportunity o start time (s) on collection asset tour ρ

$te_{ro\rho}$: imaging task r opportunity o end time (s) on collection asset tour ρ

$d_{ro\rho}$: imaging task r opportunity o duration ($te_{ro\rho}$ - $ts_{ro\rho}$) over orbit ρ

$o_{r\rho}$: imaging/collection task r opportunity o on collection asset tour ρ

$A_{ro\rho}$: area coverage request r, associated with opportunity o on collection asset tour ρ

$A_{ro\rho o'\rho'}$: overlapping area between opportunity o on collection asset tour ρ and, opportunity o' on collection asset tour ρ', associated with request r

$p_{ro\rho}$: probability of successful observation for imaging opportunity o associated with request r on collection asset tour ρ

$q_{ro\rho}$: normalized imaging opportunity o quality, associated with request r on collection asset tour ρ. $0 \leq q_{ro\rho} \leq 1$

$q_{ro\rho o'\rho'}$: mixed imaging opportunity quality associated with overlapping opportunity o and o' on related route ρ and ρ' respectively, under request r. $0 \leq q_{ro\rho o'\rho'} \leq 1$

$cost_{ro\rho}$: imaging opportunity o cost associated with request r over collection asset tour ρ

Decision variables:

$x_{ro\rho}$: binary variable indicating whether request r is serviced by imaging opportunity o on collection asset tour ρ.

The pursued objective is to maximize expected collection value (CV) allocating heterogeneous collection assets to a set of weighted/prioritized coverage, tracking and identification requests (tasks):

$$CV^* = \underset{\{x_{ro\rho}\}}{MAX} \quad CV_{TRK,CVG} + CV_{ID} \tag{1}$$

where

$$CV_{ID} \approx \sum_{r \in R_{ID}} V_{r0} \left(\sum_{\rho \in \mathrm{P}_r} \sum_{o \in O_{r\rho}} q_{ro\rho} x_{ro\rho} - \sum_{\substack{\rho \in \mathrm{P}_r\, o \in O_{r\rho} \\ (\rho,o)<(\rho',o')}} \sum \sum_{\rho'} \sum_{o' \in O_{r\rho'}} \left(q_{ro\rho} + q_{ro'\rho'} - q_{ro\rho o'\rho'} \right) x_{ro\rho} x_{ro'\rho'} \right) \tag{2}$$

$$CV_{TRK,CVG} \approx \sum_{r \in R | R_{ID} = R_{TRK} \cup R_{cvg}} V_{r0} \left(\sum_{\rho \in \mathrm{P}_r} \sum_{o \in O_{r\rho}} \left(\frac{A_{ro\rho}}{A_r} p_{ro\rho} \right) x_{ro\rho} - \sum_{\substack{\rho \in \mathrm{P}_r\, o \in O_{r\rho} \\ (\rho,o)<(\rho',o')}} \sum \sum_{\rho'} \sum_{o' \in O_{r\rho'}} \left(\frac{A_{ro\rho o'\rho'}}{A_r} p_{ro\rho} p_{ro'\rho'} \right) x_{ro\rho} x_{ro'\rho'} \right) \tag{3}$$

where

$$q_{ro\rho} = 1 - \frac{\sum_{z \in Z_o} p(z) E(\{p(h_r \mid z)\})}{E_{0r}} \qquad r \in R_{ID} \tag{4}$$

$$q_{ro\rho o'\rho'} = 1 - \frac{\sum_{z \in Z_o} \sum_{z' \in Z_{o'}} p(z) p(z') E(\{p(h_r \mid z, z')\})}{E_{0r}} \qquad r \in R_{ID} \tag{5}$$

$$E(\{p(h_r \mid Z)\}) = -\sum_{h_r \in Hyp_r} p(h_r \mid Z) \times \log_2 (p(h_r \mid Z)), \; r \in R_{ID} \tag{6}$$

$$p(h_r \mid Z) = \frac{p(Z \mid h_r) p(h_r)}{p(Z)} \qquad r \in R_{ID} \tag{7}$$

$$p(Z \mid h_r) = \left[\prod_{i=1}^{n} \left(p(z_i \mid h_r) \right) \right] p(h_r) \qquad r \in R_{ID} \tag{8}$$

$$p(Z) = \sum_{h_r \in Hyp_r} p(Z \mid h_r) p(h_r) \qquad r \in R_{ID} \tag{9}$$

$$p(z) = \sum_{h_r \in Hyp_r} p(z \mid h_r) p(h_r) \qquad r \in R_{ID} \tag{10}$$

$$p(z \mid h_r) = \sum_{s \in States} p(z \mid h_r, s) p(s) \qquad r \in R_{ID} \tag{11}$$

$$E_{0r} = -\sum_{h_r \in Hyp_r} p(h_r) \log_2 (p(h_r)) \qquad r \in R_{ID} \tag{12}$$

Collection value contribution CV_{ID} (2) for identification tasks is a second-order approximation assuming that 2-3 visits (observations) at once are deemed sufficient to obtain acceptable expected task value performance. Note that a third-order CV_{ID} approximation to achieve target identification can be further expressed through a minor extension of eq. (2) subject to an additional 3-visit constraint. Alternatively, collection value contribution $CV_{TRK,CVG}$ eq. (3) embracing basic area coverage and tracking tasks, translates a quadratic approximation of a nonlinear objective function, as few visits to specific locations composing an AOI proves quite acceptable in practice. Note that it may be also easily derived from a particular instantiation of eq. (2) expressing generic tracking imaging opportunity quality for specialized coverage and tracking tasks.

Single and mixed imaging opportunity qualities for an identification task r are modeled using an expected entropy E [5] reduction measure as shown in eq. (4)-(10). Quality reflects relative information gain over possible class membership (i.e. hypothesis $h_r \in Hyp_r$) conditional to observation outcomes z and/or z'. Entropy is captured in eq. (6) where $p(h_r|Z)$ describes class membership probability given observation outcomes Z resulting from imaging task executions, and sensor-dependent observation values $z \in Z_o$. The set of hypothesis Hyp_r defines classes of interest, such as dark/normal ship for ship identification, or low/medium/high levels for risk, behavior or threat identification. Posterior probability (7)-(9) uses Bayesian update assuming n sensor observation independence, known or simulated sensor observation model $p(z|h_r)$ and prior belief (10)-(11) on target class ownership $p(h_r)$ for that task. Initial entropy estimation is achieved using prior beliefs (12). In contrast, basic coverage and tracking task imaging opportunity quality rely on expected area coverage. Quality could alternatively be motivated by any predefined mission-specific function (e.g. kinematic error covariance on entity position). In the current setting, similarly to task-dependent imaging opportunity generation, defined track area and coverage estimations are derived from simulation and deep neural network track prediction analysis. Measures of performance parameter evaluation used to derive related quality of collection for task imaging opportunities regarding tracking and identification requests are further detailed in section 4.

3 EXTENDED GENETIC-ALGORITHM-BASED COLLECTION SCHEDULER

3.1 Description

The proposed collection scheduling algorithm generalizes the *G*enetic *A*lgorithm-based collec*T*ion sc*H*edul*ER* (*GATHER*) solution [4] initially designed for satellite platforms. Individual representation, fitness and hybrid genetic algorithm operators are adapted to accommodate heterogeneous collection assets (namely vehicles) and related resource capacity constraints. The problem-solving approach consists in evolving a mixed population of feasible/unfeasible collection plan (CP) individuals to maximize overall expected collection value. An individual is explicitly represented by a joint collection schedule (path plan) solution for each collector tour, overlooking intermediate chromosome encoding. At each generation, population composition maintains a relative proportion of separate feasible (α) and unfeasible ($1-\alpha$) subpopulation solutions to better explore the solution space and escape local extrema. The population is continuously evolved over a number of generations using genetic operators until some predefined termination conditions are met. Such conditions refer to a maximum number of generations and/or solution convergence. The latter is expressed after each generation, in terms of the best computed solution score variability over recent history (e.g., standard deviation over the past T generations)/best computed solution quality ratio. The algorithm stops when the ratio is less than a predefined threshold (e.g., 1%) over the last consecutive T generations. The initial population is built from feasible collection path solution individuals generated using a simple myopic 'maximal marginal return rate' insertion procedure, starting from an arbitrary task.

The steady-state GA can be summarized as follows:

Algorithm: GATHER

Parameters: Population size, Number of generations, rates, α

Build initial population *Pop*
Repeat
    For $i = 1..n_p$ ***do*** {new generation}
        Select two parents from *Pop*
        Randomly select a recombination or mutation operator according to rate of each operator
        Generate a new solution sol_i (mutation) or two new solutions sol_{i1}, sol_{i2} (recombination) with the selected parents and operator
        Add sol_{i1} (and sol_{i2}) to *Pop*
    end for
    Remove from *Pop* the n_p worst individuals by using the evaluation function (1)
Until (max number of generations ***or*** solution convergence)

On each generation, the algorithm inserts new solution individuals to the population until it outnumbers the initial population size by n_p solutions. The initial population size is then finally re-established rejecting the n_p worst individuals.

Designed genetic operators exploit opportunity precedence relationships, captured in collection graphs to facilitate path solution recombination and/or mutation. This allows rapidly constructing feasible collection opportunity sequences. Collection graph exploitation, and fast opportunity insertion using a simple myopic 'maximal marginal return rate' heuristic to revisit partial collection path plan, accelerates feasible high-quality solution generation.

3.2 Fitness Function

Fitness reflects the propensity of an individual solution for reproduction. Fitness derives from individual's quality, which accounts for a mixture of expected *CV* and constraint violations over resource capacity, as defined in (13) for individual *i*:

$$quality_i = CV_i - \lambda \times \begin{pmatrix} \text{average resource capacity violations per} \\ \text{non-empty/populated tour} \end{pmatrix}_i \tag{13}$$

where $\lambda = \sum_{r \in R} V_{r0}$

The normalized penalty contribution in (13) capturing tour resource capacity constraint violations is averaged over the number of scheduled tours and all related supporting resources such as energy budget, memory storage and duty cycle. Each constraint contribution is modeled as a step function approximation over anticipated path plan remaining resource level. A linear scaling scheme is finally used to rank solution individuals over quality and compute individual fitness, ensuring a more equitable selection process. Correspondingly, the fitness for individual with rank $i \in \{1,2,\ldots,|Pop|\}$ is given by:

$$fitness_i = MAX - (MAX - MIN) \times (i-1) / (|Pop| - 1) \tag{14}$$

where MAX=1.6, MIN=0.4

An individual's fitness value is negatively correlated with its ranking score. The smaller the rank the larger is its fitness value.

3.3 Selection

A roulette-wheel selection mechanism is used for reproduction purposes. The probability to select an individual is proportional to its fitness value.

3.4 Recombination

3.4.1 X_{ST} crossover. The proposed 'same tour' crossover operator X_{ST} consists of randomly selecting a tour $\rho \in P$, then recombining the respective collection path plans π_ρ and π'_ρ from two parent solutions P and P' to generate two offspring as follows: $X_{ST}(P,P')$: $P(\pi_1, \pi_2, \ldots \boldsymbol{\pi_\rho} \ldots, \pi_{|P|})$ X $P'(\pi'_1, \pi'_2, \ldots \boldsymbol{\pi'_\rho} \ldots, \pi'_{|P|})$
➔ $P^{child}(\pi_1, \pi_2, \ldots \boldsymbol{\pi^X_\rho} \ldots, \pi_{|P|})$, $P^{child'}(\pi'_1, \pi'_2, \ldots \boldsymbol{\pi^X_\rho}' \ldots, \pi'_{|P|})$

- Select crossover opportunity point o_ρ (P, π_ρ) from P's selected collection path π_ρ.

- Determine crossover opportunity point o'_ρ (P', π'_ρ) from P's selected collection path π'_ρ: earliest opportunity o'_ρ (P':π'_ρ) from π'_ρ posterior to o_ρ (P, π_ρ) end time.
- Mutually exchange respective collection subpaths from π_ρ and π'_ρ to generate corresponding child solution collection paths π^X_ρ and π^X_ρ', and repair them if required, by removing opportunity nodes violating the legal transition constraint using collection graph ρ.

The operation is illustrated in Fig. 2 for (P, P') = (Parent1, Parent2).

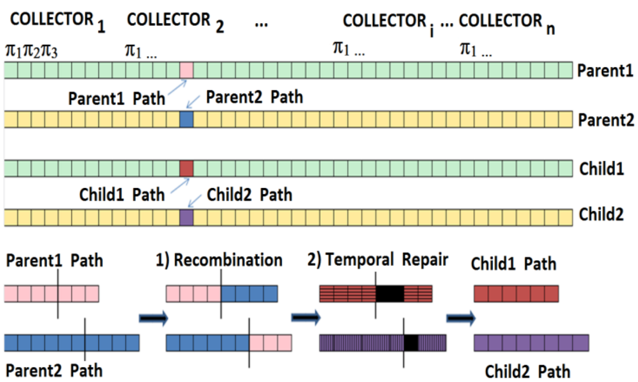

Figure 2: The "same tour" crossover operator (X_{ST}).

3.4.2 X_{TS} crossover. The alternate 'tour swap' crossover operator X_{TS} consists for a randomly selected tour ρ to exchange collection paths π_ρ and π'_ρ between two parent solutions P and P' respectively, generating two offspring P^{child} and $P^{child'}$ as follows: X_{TS}(P,P'): P(π_1, π_2,…$\boldsymbol{\pi_\rho}$…,$\pi_{|P|}$) X P'(π'_1, π'_2,…$\boldsymbol{\pi'_\rho}$ …,$\pi'_{|P|}$) ➔ P^{child} (π_1, π_2,…$\boldsymbol{\pi'_\rho}$ …, $\pi_{|P|}$), $P^{child'}$(π'_1, π'_2,…$\boldsymbol{\pi_\rho}$ …, $\pi'_{|P|}$)

If needed offspring solutions are readily repaired by eliminating low-payoff visits to meet all constraints.

3.5 Mutation

3.5.1 M_{SP} mutator. The subpath mutation operator M_{SP} randomly replaces a subpath from a parent solution, and reconnects disjoint pending head and tail path segments, therefore sequentially inserting timely feasible imaging opportunity moves selected from the collection opportunity graph. M_{SP} is shown in Fig. 3. Graph connectivity proves very convenient in efficiently repairing temporal constraint violations.

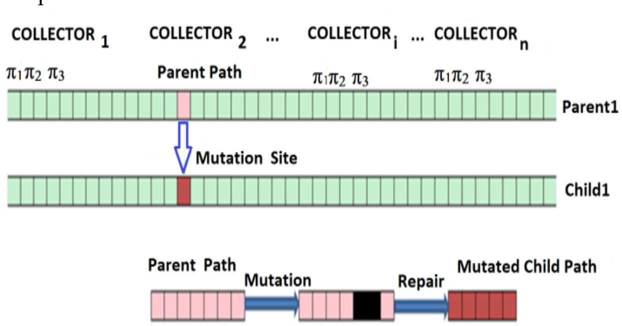

Figure 3: The "subpath" mutation operator (M_{SP}).

3.5.2 M_{FP} mutator. The full path mutation operator M_{FP} is a variant of the M_{SP} applied to a full collection path rather than being restricted to a subpath. A simple myopic 'maximal marginal return rate' insertion heuristic is used to reconstruct the path.

3.5.3 M_{REP} mutator. The M_{REP} mutator repairs unfeasible solutions resulting from constraint violations such as resource consumption exceeding capacity (e.g., memory and energy expenditure), cumulative imaging time beyond acceptable threshold (e.g. imaging duty cycle) or financial budget violation for image acquisition. As these constraint violations mostly occur toward the end of a collection path, their handling is faster (e.g. dropping low-payoff scheduled opportunities) than temporal opportunity transition breaches, likely to take place more frequently during path construction. Accordingly, a feasible parent solution can be obtained by iteratively taking away low-payoff scheduled opportunities $o(r,\rho)$ (with probability proportional to 1-$V_{r(o)0}\ p_{ro\rho}\ A_{ro\rho}/A_{r(o)}$) from an unfeasible collection path until full constraint satisfaction. The operator is used to maintain a suitable balance on individual solution feasibility when completing a new generation.

4 PREDICTION AND OPTIMIZATION

4.1 Collection Opportunities and Plan

This work utilizes a proprietary Intelligence, Surveillance and Reconnaissance (ISR) Systems Simulation Engine called Total::Perception™ which is developed and maintained by Larus Technologies Its Situational Understanding module receives anomalies that are generated by a decision support system and proceeds to perform track prediction for each member of the scenario and feeds that output to both the Contextual Awareness and Perception Management modules where various Situation Evolution Models (SEMs) are used to generate multiple future trajectories for each member with a specific probability for each of those trajectories. Each probabilistic situation is saved in a specified data store. Based on an ISR Request (ISRR), the Total::Perception™ Simulation Engine can run one or multiple situation scenarios to generate the required Collection Opportunities (COs). Once a situation-related optimal set of Collection Plans (CPs) has been iteratively generated, they are presented for the end user to visually playback for analytical purposes.

4.2 Situation Evolution Models

A Situation Evolution Model (SEM) is a model of the world (or, more realistically, a model of the dynamic aspects of some subset of the world) that will be used to predict/forecast the evolution of the current situation. That is, given some knowledge of the state of the current situation, the SEM can be used to exploit that knowledge and predict/forecast the state of this situation in the future.

Situations can change with time and evolve in certain ways based on temporal elements and circumstances with conditions in the surrounding environment. Some known example situations in the maritime domain are: drug smuggling, human trafficking, piracy, etc. Other known example situations in the land domain are: IED emplacement, kidnappings, target surveillance, etc. Each situation can evolve chronologically and pass sequentially through different states (temporal snapshots). For example, considering the situation of a piracy attack in maritime environment, and a simple pirate model in particular [6], that behaviour can be defined by multiple states: sailing, chasing, sailing away, sailing home, sailing home with hijacked ship, waiting for ransom, etc.

The generation of a SEM requires deep knowledge of the domain of that situation and of the dynamics of that domain, in addition to related subsets of interest of the world. Subject matter experts (SMEs) can determine a SEM related to their domain(s) of experience. Then, a predictor can be custom designed in a way that can learn the behaviour of that SEM. Machine learning can be used to train a predictor that can learn the evolution process of such SEMs. This will enable the system to provide a probability distribution over multiple future evolutions. Henceforth, the system can exploit these various options all at once and provide the end user with clearer probabilistic picture of what could occur.

Different kinds of SEMs can be defined, addressed, and categorized as kinematics-based, threat-based, risk-based, and objective-based. In this work, we will focus on the former two as they are quite suitable for track prediction in high-level data/information fusion systems. Using these models, one can feasibly generate space-time COs over a given time window, ultimately leading to the selection of an optimal CP among multiple possible opportunity combinations.

4.2.1 Kinematics-Based SEM. In this section, we propose the use of a Long-Short Term Memory Recurrent Neural Network (LSTM-RNN) to forecast a vessel track based on kinematic Automatic Identification System (AIS) features such as Speed, Lat, Long, True Heading. The proposed LSTM-RNN with 10 feature lags architecture is provided in Fig. 4 where each LSTM unit is composed of gates. The LSTM-RNN architecture consists of seven stacked layers, layer 1 has 512 LSTM units, layer 2 has 256 LSTM units, layer 3 has 128 LSTM units, layer 4 has 64 LSTM units, layer 5 has 32 LSTM units, layer 6 has 16 LSTM units, and layer 7 is a dense layer with four outputs to forecast Speed, Lat, Long, True Heading. The LSTM- RNN is trained on January and February of 2018 real-world AIS data and then is given part of the track and asked to forecast the normal track of a tanker as shown in Fig. 5 where the green points are the forecasted track whereas the red points are the ground truth from AIS data.

4.2.2 Threat-Based SEM. This SEM is a lot more abstract and complex where many factors determine the evolution of the model. Examples of these factors include: location characteristics, distance from certain points of interest (e.g. natural choke points, fishing zone, enemy air defence areas, maritime borders, shallow waters, etc.), time, and object under threat specifications, physical activities in the surroundings of threatening objects, area history of hostility, neighbouring countries' political instability, geographical data and historical data about the situation environment in the surrounding location of interest. Current and prior states' hard (i.e. structured) data, along with a history of soft (i.e. unstructured) data, are fused together to train a predictor that can predict a threat to occur in the future. To build this kind of SEM, an advanced Recurrent Neural Network (RNN) architecture was custom designed to suit a certain individual SEM and to learn its evolutionary states such that different type of inputs and outputs were created. Fig. 6 shows a generic block diagram of the prediction task that learns a particular SEM's behaviour. The situation at the current discrete time *S(k|k)* and its state history are provided as inputs to the predictor. These inputs can have hard and soft data to form feature vectors to train the predictor.

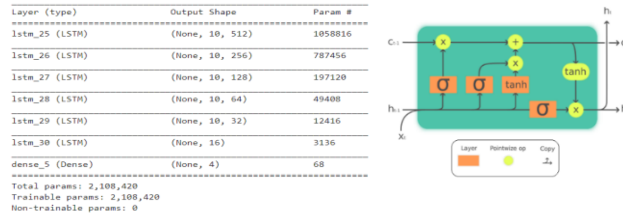

Layer (type)	Output Shape	Param #
lstm_25 (LSTM)	(None, 10, 512)	1058816
lstm_26 (LSTM)	(None, 10, 256)	787456
lstm_27 (LSTM)	(None, 10, 128)	197120
lstm_28 (LSTM)	(None, 10, 64)	49408
lstm_29 (LSTM)	(None, 10, 32)	12416
lstm_30 (LSTM)	(None, 16)	3136
dense_5 (Dense)	(None, 4)	68

Total params: 2,108,420
Trainable params: 2,108,420
Non-trainable params: 0

Figure 4: LSTM architecture (left) and single unit (right) with 10 lag features

Figure 5: Ground truth tanker route (red) and the LSTM forecasted track (green)

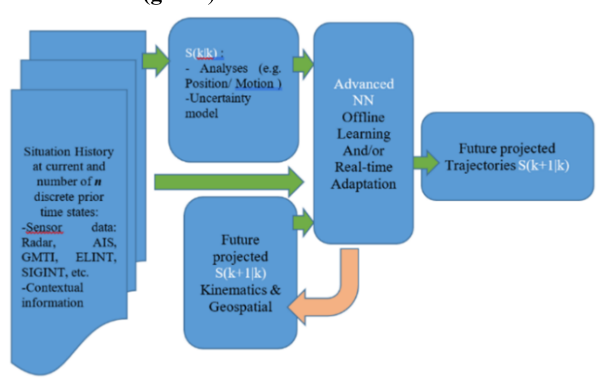

Figure 6: Threat-based SEM RNN-based predictor

In general, all the designed SEMs have an RNN with 2 input layers with different delay lines (e.g. 1:5, 0:50), multiple hidden layers; one output layer, and a feedback delayed line from the output to the input layers. Training, verification, and testing were considered to prevent the overfitting and aim for a generalization of the predictor. Fig. 7 shows a snapshot of simulated run of a trained pirate behaviour SEM that learned to intercept a maritime vessel. This behaviour is used to predict future trajectories for a period of time expected to demonstrate the threatening attitude.

Figure 7: Pirate behaviour predicted by the threat-based SEM. Pirate is in green while the victim is in white

The threat-based SEM's RNN has a sliding window vector as an input consisting of shifts of latitude and longitude, heading changes, heading/distance to the vessel of interest (VOI), both speeds of pirate and VOI, time intervals, etc. The output is the distance and heading to the future predicted locations. Fig. 8 shows the actual track at the prediction point as well as the rendezvous scenario where an SEM predictor learned to predict the future trajectories of 2 vessels: a Tanker vessel and another vessel coming from Port George in Prince Edward Island (PEI).

4.3 Identification

A task-specific knowledge-based identification system mimicking a subject matter expert coupled to Monte Carlo simulations is currently assumed to estimate class membership (e.g. ship identification, risk estimation) probability distribution for a given collection plan. Domain knowledge are mainly captured from user experience and inspired from National Imagery Interpretability Rating Scale (NIIRS) [7] standards as well as sensor performance models for optical imaging systems [8]. The latter include the discrimination probability (detection, recognition, identification) model, and General Image Quality Equation [9] promoted by the Imagery Resolution Assessment and Reporting Standards (IRARS) Committee. Single and mixed imaging opportunity qualities are estimated using entropy reduction measure based on average collection plan (imaging opportunity combinations) performance simulations or known (assumed) observation models.

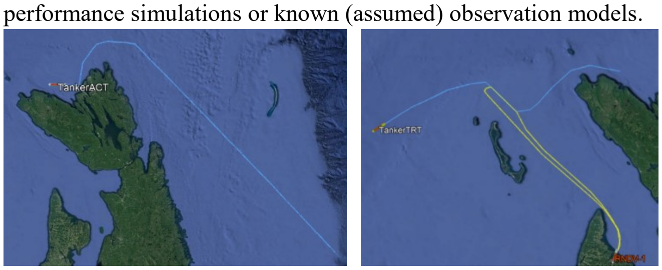

Figure 8: Original track at prediction point and predicted behaviour of a rendezvous

5 EXPERIMENTAL RESULTS

A fictitious scenario was synthesized for the purposes of this paper whereby a tanker (i.e. AIS type 80) traversing the Atlantic and entering the St. Lawrence was selected as the VOI. The latter's current trajectory was sent to both the kinematics-based and threat-based SEMs to generate two predicted trajectories. These form the dynamic paths that are sent to the optimization models which, in turn, generate the space-time COs for the temporal window of the prediction, and to the selection of an optimal CP among the two trajectories. The assets that are employed in the surveillance task of this dynamic track include an Unnamed Aerial System (UAS), an aircraft typically used for surveillance in addition to spaced-based assets; all these platforms, as well as their on-board sensors, were modeled to perform the asset movements and surveillance taskings.

5.1 Scenario

Fig. 9 demonstrates the threat-based SEM including the trajectory of the 2 vessels involved in the rendezvous as well as the 2 airborne surveillance assets performing rectangle racetrack and snake-like surveillance patterns in order to achieve detections of the scenario actors, as well as a detection by one of the space-based assets that were included in the surveillance task of these dynamic tracks.

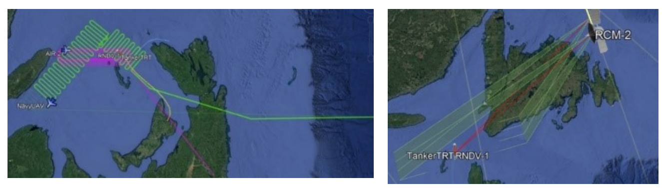

Figure 9: Threat-based SEM with 2 airborne surveillance (left) and space-based surveillance (right) assets

6 CONCLUSION

A new framework combining discrete-event simulation, deep neural networks and evolutionary approach has been proposed to solve multi-asset collection/image acquisition scheduling in a surveillance context. From an extended decision model incorporating coverage, tracking and identification tasks, it generalizes a graph-based hybrid genetic algorithm used for satellite scheduling assuming heterogeneous collection asset/vehicles such as air and ground-based vehicles subject to a mixture of capacity constraints. The framework relies on a predictive simulation-based deep neural network capability to generate and select tracks/behaviors and a predefined knowledge-based approach in feeding tracking and identification task decision model performance parameters.

Future work consists in further enhancing probabilistic classifiers exploiting deep learning coupled to Monte Carlo simulation to fully automate and assess tracking and identification task plan performance.

REFERENCES

[1] Chen, X. et al. 2018. Priority-based and conflict-avoidance heuristics for multi-satellite scheduling, Applied Soft Computing 69, 177–191.
[2] Song, Y., Huang, D., Zhou, Z. et al. 2018. An emergency task autonomous planning method of agile imaging satellite. EURASIP J. on Image and Video Proc. (29), 2-11.
[3] Wang J., Demeulemeester E., Qiu D. and Liu J. 2015. Exact and Inexact Scheduling Algorithms for Multiple Earth Observation Satellites under Uncertainties of Clouds. Available at SSRN: https://ssrn.com/abstract=2634934.
[4] Berger, J., Giasson, E. et al. 2018. A Graph-based Genetic Algorithm to Solve the Virtual Constellation Multi-Satellite Collection Scheduling Problem, IEEE Congress on Evolutionary Computation, Rio de Janeiro, Brazil.
[5] T. Cover, J.T., 2006. Elements of Information-Theory, 2nd edition, Wiley.
[6] Michal Jakob, "Adversarial Modeling and Reasoning in the Maritime Domain Year 2 Report," December 31, 2010.
[7] John M.I. 2001. National Imagery Interpretability Rating Scales (NIIRS): Overview and Methodology, Proceedings of SPIE, Vol.3128, 93-101.(2001)
[8] Kang, S. and al. 2014. A Study on Correlation between National Imagery Interpretability Rating Scale and Discrimination Probability. International Symposium on Optoelectronic Technology and Application 2014: Optical Remote Sensing Technology and Applications, edited by Anatoli G. Borovoi, Dong Liu, Proc. of SPIE Vol. 9299, 92991B
[9] Steve A. C., Christopher J. F., David J. D. 2009. The Use of the General Image Quality Equation in the Design and Evaluation of Imaging Systems. Proc. of SPIE Vol. 7458.